Structure and energetics of polyhydroxylated carbon fullerenes

J. G. Rodríguez-Zavala*
Instituto de Física "Manuel Sandoval Vallarta," Universidad Autónoma de San Luis Potosí, Alvaro Obregón 64, 78000 San Luis Potosí, México

R. A. Guirado-López†
Instituto de Física "Manuel Sandoval Vallarta," Universidad Autónoma de San Luis Potosí, Alvaro Obregón 64, 78000 San Luis Potosí, México
and Programa de Ingeniería Molecular, Instituto Mexicano del Petróleo, Lázaro Cárdenas 152, 07730 México D.F., México

(Received 31 March 2003; revised manuscript received 18 September 2003; published 23 February 2004)

We have performed semiempirical modified-neglect-of-diatomic-overlap (to determine the most stable geometrical arrangements) as well as *ab initio* density-functional theory calculations (to obtain the electronic structure and total energies) at $T=0$ to analyze the energetics and structural properties of OH species adsorbed on the external surfaces of spheroidal C_{60} as well as on finite length open-ended armchair (6,6) and (8,8) carbon nanotubes. Interestingly we have found, for the low coverage regime, that the adsorbed OH groups prefer to organize as a hydroxyl cluster (having up to seven OH molecules) in only one side of the C_{60} surface. The observed clustering leads to the formation of a new amphiphilic molecule that naturally explains the stability of $C_{60}(OH)_n$ ($n\sim$9-12) Langmuir monolayers at the air-water interface observed by several authors, where it is thus only the highly hydroxylated part of the carbon cage the one that dissolves in water slightly. For 8 to 14 adsorbed OH groups, a second hydroxyl island is gradually stabilized on the opposite side of the carbon structure, and finally, with increasing coverage the coexistence of ringlike and cluster arrays of OH groups seems to lead to the complete solubility of the carbon compound. In all cases, the OH molecules have been found to occupy on-top sites with a C-O-H bond tilted away from the surface normal and no hydrogen bond formation between the adparticles is obtained, in contrast to what is normally observed in the compact OH hexagonal phases stabilized on extended metal substrates. The calculated vibrational frequencies of our adsorbates have a good correspondence with the experimental measurements and provide a clear signature of the clustering of the OH molecules at low coverages. Finally, OH adsorption on the external surface of cylindrical carbon structures leads to the formation of quasi-one-dimensional molecular arrays, consistent with the synthesis of metal nanowires on the surface of carbon nanotubes, their length being determined by the length of the nanotube.

DOI: 10.1103/PhysRevB.69.075411 PACS number(s): 61.48.+c, 73.22.−f, 72.80.Rj

I. INTRODUCTION

In the last years, the possibility of fabricating a new generation of materials based on the assembly of individual carbon nanostructures has attracted considerable attention. In particular, both macroscopic arrays made of C_{60} molecules and carbon nanotubes have been found to be excellent candidates towards the synthesis of novel materials with controlled properties. Although a wide variety of technological applications rely on the pure carbon structures, it is well known that interesting phenomena have been obtained also for fullerene-doped compounds. For example, in the case of carbon nanotubes, it has been suggested that encapsulation of magnetic materials could develop giant coercitivities which would make possible their use as very high-density recording media.[1] Recently, Gao and Bando[2] have demonstrated that carbon nanotubes filled with gallium can be also used for temperature measurements in microenvironments. In addition, their different electrical response upon gas adsorption (e.g., NH_3 and NO_2) seems to offer the possibility of using them as chemical sensors as well as tunable molecular conductors[3] and finally, their large empty space has suggested additional applications as gas (e.g., H_2 and N_2) storage materials.[4] In the case of spheroidal fullerenes, interesting experimental data can be also found in the literature. It is already well known that the interaction of solid C_{60} with some alkaline elements can lead to superconducting materials.[5] Furthermore, their use as photoactive molecular systems has been recently discussed,[6] being particularly important for the conversion of solar energy into electric current. The fabrication of ordered two-dimensional arrays and multilayered structures of C_{60} molecules in solid surfaces[7] or at air-water interfaces[6,8,9] has revealed interesting optical and transport properties and finally, the encapsulation of atoms such as Gd in the C_{82} fullerene can provide an improved contrast-enhancing agent for magnetic-resonance imaging,[10] or in the case of radioactive atoms such as holmium, effective tracers, or anticancer agents can be produced.[11]

The fundamental problem with the last two types of applications mentioned here above, which could have important implications in the fabrication of electronic devices [synthesis of C_{60}(organic-group)$_n$ monolayers at the air-water interface which can be later on transferred to solid substrates] and medical diagnoses [endohedral (Gd,Ho)@C_{82} compounds], is strictly related to the extreme hydrophobicity of pure carbon fullerenes. In order to solve this problem, coating of some spheroidal carbon structures (e.g., C_{60} and C_{82}) with a wide variety of water-soluble organic molecules

has become a typical experimental procedure.[6,8,10] To date, the substituents of choice to produce water solubility have been either hydroxyl or carboxylic groups. Interestingly, when using OH molecules, it has been found that the degree of solubility (partial or total) of the fullerene-$(OH)_n$ compounds critically depends on the number of OH's attached. For example, Liu *et al.*[8] have reported that 12 hydroxy groups bounded to the C_{60} cage provide the adequate hydrophobic-hydrophilic balance to stabilize $C_{60}(OH)_{12}$ Langmuir monolayers at the air-water interface. Similarly, Rincón *et al.*[9] have obtained stable Langmuir films with the use of $C_{60}(OH)_{\sim 9-12}$ units. However, it is well known that, with increasing OH coverage, completely water-soluble fullerenes can be obtained. This is particularly the case of the $C_{60}(OH)_{24-28}$ compounds[9] as well as of the endohedrally doped $Gd@C_{82}(OH)_{40}$ structure.[10] Although, in the experimental setup it is possible to estimate the average number of adsorbed OH's by means of mass spectrometry experiments (e.g., matrix-assisted laser desorption ionization technique), it is very difficult to identify the geometric structure of the various adsorbed phases that can be stabilized as a function of coverage and characteristics of the underlying substrate, and which are obviously at the origin of the observed chemical and physical properties in these materials over a large scale, e.g., it has been found that macroscopic samples of highly hydroxylated C_{60} molecules give a dielectric structure, while materials with low levels of hydroxylation result in proton conductive compounds.[9]

As is well known, single-wall carbon nanotubes (SWNT's) can be also used as substrates for deposition of various metals or molecules by evaporation techniques. Actually, it is well known that a carbon nanotube with adsorbed materials may also significantly change its physical properties, providing thus useful means for manipulating electronic transport for nanoelectronic devices. At this respect, it is important to comment that recent experimental and theoretical studies have demonstrated that even small amounts of gas molecules such as NH_3 and NO_2 (Ref. 3) adsorbed on the external surface of a cylindrical carbon structure have a significant effect on its electrical transport characteristics. Furthermore, carbon nanotubes can be functionalized with a wide variety of molecular species to be made soluble in common solvent systems, offering thus the opportunity also to study the complex nanotube-molecule interactions in homogeneous solution.[12] In particular, with the help of surfactants, it has been found that short length carbon nanotubes can form stable colloidal suspensions in water, permitting a variety of manipulations, such as separation by length, derivatization, and tethering to specific surfaces.[13]

Previous experiments considering the interaction of OH groups with extended metal substrates have demonstrated that, as a function of temperature and coverage, various adsorbed phases can be obtained. In particular, a combined high-resolution electron energy loss spectroscopy and scanning tunneling microscopy (STM) study of OH adsorption on the Pt(111) surface[14] has demonstrated the existence of ordered OH hexagonal arrays, their formation being driven by the formation of hydrogen bonds between the neighboring hydroxyl molecules. In these cases, it is well known that a delicate balance between the competing intermolecular and molecule-surface interactions defines the adsorbates' self-organization and packing, and that both type of interactions critically depend on the chemical and geometrical details of the substrate. It is thus reasonable to expect a contrasting bonding behavior when small molecules are adsorbed on metallic or semiconducting materials, on bare surfaces or in the presence of coadsorbed species, or when deposited on two-dimensional extended substrates or three-dimensional curved surfaces as the ones exposed by fullerene materials.

In this work, we present thus a systematic study, by combining both accurate semi-empirical [modified-neglect-of-diatomic-overlap (MNDO)] as well as *ab initio* density-functional theory (DFT) approaches, in order to obtain the electronic and structural properties of polyhydroxylated carbon fullerenes. To analyze the influence of the geometrical details of the carbon substrate in the local organization of the OH molecules we will consider both spheroidal C_{60} as well as cylindrical armchair (6,6) and (8,8) nanotubes. The maximum coverage θ (defined as the ratio of adsorbed molecules to surface atoms) on the carbon surfaces is far below a complete monolayer (up to $\theta \sim 2/3$), however it has been found to be enough to understand the sizable variations observed in the water solubility between low and highly hydroxylated C_{60} structures. The vibrational frequencies of our $C_{60}OH_n$ compounds, which are expected to depend sensitively on the number and distribution of the adsorbed hydroxyl molecules as well as on the interactions among them, will be calculated in order to compare with recent experimental measurements.[9] The rest of the paper is organized as follows. In Sec. II we briefly describe the theoretical models used for the calculations. In Sec. III we present our results analyzing the structural aspects and the electronic behavior and finally, in Sec. IV the summary and conclusions are given.

II. METHOD OF CALCULATION

The number of atoms involved in our considered systems (up to ~ 200) limits the applicability of DF optimization-based methods and that is why we have decided to perform our systematic study by combining two different theoretical approaches. In a first step, we have fully optimized the considered structures using the semiempirical MNDO level of theory[15] and then, in a second step, we have used these MNDO geometries to perform single-point *ab initio* DFT calculations considering in the latter the local-density approximation (LDA).[16] On the contrary, only when determining the vibrational frequencies of some relevant examples, the total energy as well as the electronic and ground-state structure of our OH-coated fullerenes will be obtained within the same theoretical framework by performing a fully DFT geometry unrestricted energy minimization procedure with the use of the most accurate generalized gradient approximation (GGA) for the exchange-correlation potential. In this case, the Kohn-Sham equations are solved by considering the nonlocal Becke's three-parameter exchange functional[17] combined with Lee, Yang, and Parr's correlation functional[18] (B3LYP).

We must say that our considered hybrid procedure could

be justified since the accuracy of the MNDO method has been proved in several calculations of fullerenes and fullerene-derived materials. For example, for the C_{60} molecule MNDO finds bond lengths of 1.474 and 1.400 Å,[19] for single and double bonds, respectively, in good agreement with gas phase electron studies [1.458 ± 0.006 Å and 1.401 ± 0.010 Å (Ref. 20)] and *ab initio* calculations (1.446 Å and 1.406 Å).[21] MNDO calculates the ionization potential of C_{60} to 8.95 eV,[19] slightly larger than the values obtained from *ab initio* calculations [7.92 eV (Ref. 22)] and experiment [7.56–7.62 eV (Ref. 23)] and finally, doped fullerenes [e.g., Li_xC_{60} ($x=0,\ldots,14$) (Ref. 24)] and large carbon clusters[19,25] have also been successfully studied using the MNDO approximation.

The electronic structure and total energy of the molecules are obtained by means of the GAUSSIAN98 software[26] where the molecular orbitals are expanded as a combination of Gaussian functions centered at the atomic sites, and the exchange-correlation effects can be treated within the density-functional scheme. In particular, the Kohn-Sham equations are solved by considering the local-density approximation. We use the STO-3G basis[27] (STO—Slater-type orbital) which is a minimal set that is formed by fixed-size atomic-type orbitals. The STO-3G considers three Gaussians per basis function, for example, in a carbon atom we have three Gaussians which are a least-squares fit to a Slater $1s$ orbital, and we have also another three Gaussians which are a least-squares fit to Slater $2s$ and $2p$ orbitals. Obviously, larger basis sets approximate more accurately the orbitals by imposing fewer restrictions on the location of electrons in space. As a consequence, in order to illustrate the dependence of results on the choice of basis functions, we have done some calculations by using a more extended set, 6–21G.[28] The calculations, which involved a higher numerical effort, are found to lead essentially to the same conclusions.

The numerical accuracy of the method is tested by calculating some well-known properties of the C_{60} molecule. We obtain for the previously optimized MNDO structure, by using the local-density approximation together with the minimal STO-3G basis set, that the occupied electronic states fall within a range of ~ 21 eV and that the energy difference between the highest occupied molecular orbital (HOMO) and lowest unoccupied molecular orbital (LUMO), Δ_{HL}, is of 2.14 eV, both results being in satisfactory agreement with more sophisticated calculations.[29] On the other hand, we must say that our results are underestimated when compared with experimental measurements[30] performed on C_{60} thin films (HOMO-LUMO energy gap of 2.3 eV and valence-band width of 23 eV), where solid-state effects such as ordering of the molecules and shrinkage of the cluster lattice are known to produce sizable modifications in the electronic spectra. We found, for the C_{60} molecule, a binding energy E_b of 12.1 eV/at (where at stands for atom) which is overestimated with respect to the reported values in the literature, however, as is well known, this corresponds to a basis set effect. Actually, the same LDA calculation but using the more extended 6–21G basis gives a reduced value for E_b by almost 2 eV (10.3 eV/at). Despite these observed sizable variations in the absolute values of E_b for different basis sets, it is important to comment that energy differences within both type of calculations are almost the same (see the results in Sec. III) and as a consequence, in the following, only relative values are important.

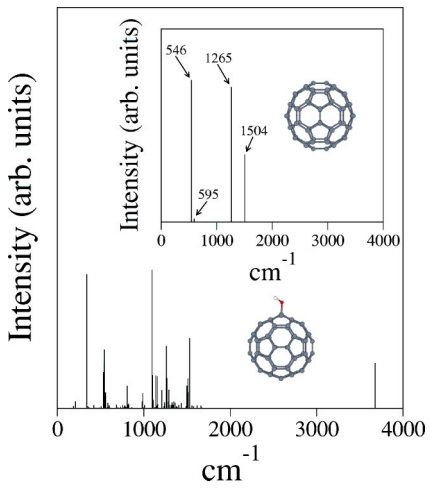

FIG. 1. Intensities of calculated vibrational frequencies for C_{60} (inset) and $C_{60}OH$ structures.

To further assess the reliability of our considered methodology we have analyzed also the interaction of a single OH molecule with the external surface of the C_{60} fullerene. From our calculations we have found that the MNDO lowest-energy atomic array corresponds to the OH group directly adsorbed on top of a carbon atom of the fullerene cage through the oxygen atom, having C-O and O-H bond lengths of 1.38 and 0.95 Å, respectively, together with a C-O-H angle of 112.3°. The previous structural parameters are in satisfactory agreement with the ones obtained by considering the electronic and geometrical degrees of freedom within the same DFT-B3LYP approach, where values of 1.48 and 1.03 Å are found for the C-O and O-H bond lengths, respectively, together with a C-O-H tilting angle of 101.3°.

Finally, the intensities of the vibrational frequencies of both C_{60} and $C_{60}OH$ structures have been also obtained. In this case, the diagonalization of the full Hessian matrix within the harmonic approximation (i.e., considering the matrix of all second derivatives of the total DFT-B3LYP electronic energy with respect to Cartesian nuclear coordinates) is performed. This procedure generates all vibrational modes of the molecular structure under consideration which can be directly related with experimental infrared (IR) spectroscopy measurements. From Fig. 1 we can see that, for the C_{60} structure (see the inset), we have found the existence of well-defined peaks at 546, 595, 1265, and 1504 cm^{-1} which are in good agreement with the absorption bands normally observed in the IR spectrum of the C_{60} fullerene[9] located at 526, 576, 1182, and 1428 cm^{-1}. From Fig. 1 we can appreciate also that a more complex distribution of vibrational modes for the $C_{60}OH$ compound is found because of the lower symmetry of the carbon structure obtained (i.e., higher number of inequivalent sites, of different bond lengths, as well as of different angles between the bonds connecting nearest-neighbor atoms) upon single OH adsorption. As ad-

ditional features to the pure fullerene cage, significant C-O and O-H stretching contributions in the $C_{60}OH$ spectra should be observed. The former is located around 1000 cm^{-1}, however it is surrounded by a complex mixture of various bond-stretching and angle-bending contributions of the carbon cage around that frequency range, while the latter is directly reflected by the presence of an isolated peak centered at 3676 cm^{-1}. We must say that both contributions are in agreement with the positions of well-defined absorption bands in the IR spectra of $C_{60}(OH)_{24-28}$ compounds assigned to C-O (1070–1090 cm^{-1}) and O-H (3430 cm^{-1}) stretching modes,[9] clearly reflecting thus the formation of the $C_{60}OH$ complex.

All these previous findings suggest that our theoretical approach will reasonably describe the stability and electronic properties of OH-fullerene compounds. However, at this respect, it is important to precise also that our considered hybrid methodology will certainly affect the quality of the calculated total energies. It is expected that our semiempirical approach used for obtaining the lowest-energy atomic arrays will give reduced values for the interatomic distances when compared with more sophisticated theoretical calculations (as already shown in the previous paragraph) and experimental data. Furthermore, due to the well-known tendency of the LDA to overbinding together with the minimal basis set considered in the calculations, we expect to approach the real binding energies of our OH-coated fullerene structures from above.

III. RESULTS AND DISCUSSION

In the following sections, we present our results for the structural, electronic, and vibrational properties of spheroidal C_{60} and cylindrical armchair (6,6) and (8,8) nanotubes passivated with OH molecules. Unless explicitly specified, all calculations will be performed using the two-step MNDO/DFT-LDA hybrid methodology. It is important to comment that the semiempirical MNDO geometry optimization scheme is orders of magnitude faster than *ab initio* methods and easily allows us to perform a systematic spin and geometry unrestricted energy minimization procedure, the former being necessary when an odd number of adsorbed OH molecules is considered. We must say that for all values of θ, several initial configurations, as the ones shown in Fig. 2, were considered, namely, (1) randomly distributed on the surface [Fig. 2(a)], (2) aggregated on one side of the C_{60} molecule [Fig. 2(b)], and (3) forming various $(OH)_n$ hydroxyl clusters of different sizes and with varying spatial distribution on the carbon structure [Figs. 2(c) and 2(d)]. In all cases, the individual OH molecules are initially placed on top of a C atom of the fullerene cage at a C-O bonding distance of 1.4 Å and forming a C-O-H angle of 180°. Then, in a second step, a complete symmetry unconstrained minimization calculation is performed. At this point, it is important to comment that different adsorption sites may develop as a function of coverage and initial configuration of the adsorbates since the bonding between the OH group and the carbon network could be altered by the effect of neighboring hydroxyl molecules. Although we are confident that low-energy configurations have been obtained, we do not in any way presuppose that these are global minima of their potential-energy surfaces. In this work we do not attempt to perform an extensive exploration of all resulting $(OH)_n$-C_{60} isomers, but instead to try to reveal more general tendencies concerning the electronic structure, intermolecular interactions, and stability of these compounds.

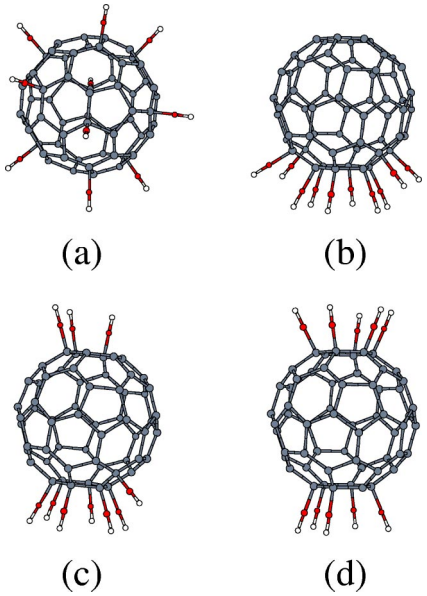

FIG. 2. Schematic view of some of the considered initial configurations of $C_{60}(OH)_N$ compounds for $N=10$. (a) OH molecules randomly distributed on the surface, (b) clustered on one side, and forming (c) two opposite $(OH)_7$ and $(OH)_3$ as well as (d) $(OH)_5$ and $(OH)_5$ clusters on the carbon structure.

A. OH adsorption on spheroidal C_{60}

In Fig. 3, we present first our calculated MNDO lowest-energy atomic configurations for $C_{60}(OH)_n$ fullerene compounds at low coverages ($0 \leqslant n \leqslant 14$). The low hydroxylated structures are important to analyze since they have been found to be still insoluble in water, currently used in the formation of $C_{60}(OH)_n$ Langmuir films at the air-water interface, and subject of controversy with respect to the possible molecular organization of the OH species on the carbon surface. From Fig. 3(a) we can see that, as already stated in the preceding section, the lowest-energy array for the single OH adsorption corresponds to the hydroxyl molecule directly adsorbed on top of a carbon atom of the fullerene cage having C-O and O-H bond lengths of 1.38 and 0.95 Å, respectively, and tilted away from the surface normal with a C-O-H angle of 112.3°. Actually, we must say that, when starting with configurations in which the OH molecule is located over C-C bonds or above the center of hexagonal and pentagonal rings, we have observed lateral displacements of the hydroxyl group in order to stabilize the on top configuration. It is important to remark that the adsorption of a single OH molecule has a negligible effect on the global shape of the carbon cluster, however, we find sizable modifications in the C-C bonds in the proximity of the OH group. The nearest-

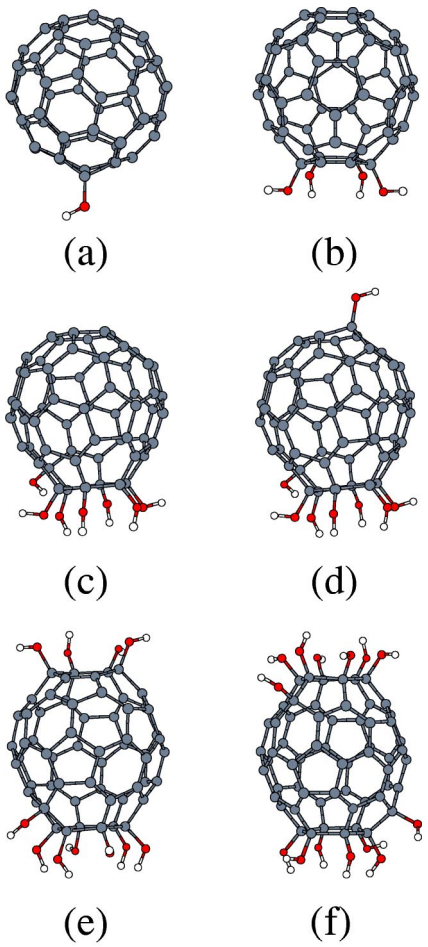

FIG. 3. Calculated (MNDO) lowest-energy structures for low hydroxylated $C_{60}(OH)_N$ compounds ($1 \leqslant N \leqslant 14$). (a) $C_{60}OH$, (b) $C_{60}(OH)_4$, (c) $C_{60}(OH)_7$, (d) $C_{60}(OH)_8$, (e) $C_{60}(OH)_{11}$, and (f) $C_{60}(OH)_{14}$.

neighbor distances in the carbon surface vary between 1.39 and 1.56 Å, the largest expansions ($\sim 10\%$) being between the carbon atoms closer to adsorption site. Finally, it is important to comment that OH bonding induces a notable redistribution of charge in both the hydroxyl molecule and on the C_{60} cage. Actually, the carbon atom directly involved in the bonding loses a total of $0.1\bar{e}$, which have been found to be transferred not only to the OH group but also to the carbon atoms around the adsorption site.

We have calculated the adsorption energy E_{ads} defined as

$$E_{\text{ads}}(C_{60}-n\text{OH}) = -[E_t(C_{60}+n\text{OH}) - E_t(C_{60}) - nE_t(\text{OH})]/n, \qquad (1)$$

where $E_t(C_{60}+n\text{OH})$ and $E_t(C_{60})$ are the total energies of the C_{60} with and without n OH molecules attached, respectively, and $E_t(\text{OH})$ is the total energy of an isolated OH molecule. For the adsorption of a single OH [$n=1$ in Eq. (1)], we have obtained a value for E_{ads} of 2.5 eV, which clearly indicates that this molecule undergoes chemical adsorption on the C_{60} fullerene. In addition, a binding energy E_b of 11.9 eV/at is obtained for the C_{60}-OH structure. From this value for E_b we can see that our OH-fullerene compound is stable however, it is less favorable (by 0.2 eV/at) when compared to uncoated C_{60}. At this point, it is interesting to compare the previous results found for the relative stability with the ones obtained by using the more extended 6–21G basis. With the more accurate set we have found, as expected, reduced values for E_b of 10.3 and 10.1 eV/at for C_{60}, and C_{60}-OH, respectively. Notice also that, when compared with the STO-3G calculations, the same energy ordering is obtained, being again our $C_{60}OH$ structure less stable by 0.2 eV/at with respect to the uncovered carbon cage. Finally, we have found a HOMO-LUMO energy gap Δ_{HL} of ~ 0.34 eV (very close to the value of ~ 0.25 eV obtained with the 6-21G basis) which is considerably reduced when compared to the one obtained in the uncovered cage ($\Delta_{\text{HL}}=2.14$ eV). This sizable reduction in the energy gap is due to the appearance of several additional electronic states around the Fermi level of our complexes, which are induced by the presence of the adsorbed OH groups. These additional states are mainly of oxygen $2p$ character, and are found to be coupled with the valence $2p$ states of the carbon atoms of the fullerene cage, a fact that shows that the transport properties of C_{60} can be modified by the bonding of the hydroxyl molecules.

The previous results have already revealed interesting features concerning the structural and electronic aspects of single OH adsorption on the external surface of the C_{60} fullerene. However, it is clear that additional interesting phenomena are expected with increasing OH coverage where not only the relevant molecule-surface bonding features (already discussed in the previous paragraphs) but also the intermolecular OH-OH interactions will start to play a key role in defining the distribution of adsorbates on the surface, as well as the electronic properties of the fullerene compounds.

From Figs. 3(b)–3(f) we can see that, with increasing the number of OH's attached, the local organization of the adsorbates on the C_{60} surface is highly θ dependent and that, even for our highest coverages (up to 32 adsorbed OH groups), no hydrogen bond formation, as in the case of OH adsorption on Pt(111) surfaces,[14] is observed (see Fig. 8). From Figs. 3(b) and 3(c) we note that, in the low coverage regime (from two to seven adsorbed species), a molecular hydroxyl cluster is stabilized on one side of the carbon surface, where the OH groups prefer to adsorb on adjacent carbons of the fullerene network forming a hexagonal disconnected array. The molecular structure shown in Fig. 3(c) is particularly interesting since it is characterized by the presence of a localized hydrophilic environment which, as we will see in the following, could be of fundamental importance in explaining the formation of low hydroxylated C_{60} monolayers at the air-water interface.[8,9] Interestingly, when attaching an additional OH group to the fullerene cage to form the $C_{60}(OH)_8$ compound, we found that the largest energy gain is obtained when the extra hydroxyl molecule is now located on the opposite side of the carbon structure [see Fig. 3(d)]. The previous result is very important since it defines a critical size for the molecular hydroxyl cluster that can be stabilized on the fullerene surface, reveals the existence of competing effects which can induce molecular aggregation or significant displacements of the adsorbates as a

function of θ, and clearly shows also that OH adsorption on C_{60} is considerably affected by the presence of coadsorbed species. Finally, from 9 to 14 adsorbed molecules [see Figs. 3(e) and 3(f)], we have not observed a dramatic reorganization of the OH groups but instead the continuation of a well-defined growth sequence in which a second hydroxyl island is gradually stabilized on the opposite side of the fullerene cage, a fact that induces the development of a highly anisotropic underlying carbon network being driven by sizable vertical as well as lateral shifts of the carbon atoms around the adsorption sites [e.g., Fig. 3(f)].

It is clear that the existence of molecular hydroxyl islands on the surface of the C_{60} fullerene, as the ones shown in Fig. 3, leads to the formation of new amphiphilic molecules that, as previously stated, could be very helpful in explaining the stability of $C_{60}(OH)_n$ ($n \sim 9-12$) Langmuir monolayers at the air-water interface observed by several authors. Despite the existence of a large number of studies addressing the solubility of the C_{60} molecule, it has been always difficult to elucidate the precise geometric structure of the adsorbed hydroxyl phases that can be stabilized on the surface of such small objects and that could lead to a wide variety of macroscopic behaviors. In particular, Chiang and co-workers[8] have obtained adsorbed $C_{60}(OH)_{12}$ monolayers at the air-water interface, whose characterization indicated 12 hydroxy groups randomly bounded on the C_{60} cage. On the other hand, Rincón and co-workers[9] have synthesized also low hydroxylated C_{60} Langmuir films where their data suggest, contrary to the work of Chiang *et al.*, that 9–12 hydroxy groups seem to be preferentially bounded on one side of the C_{60} cage. To support their assumption, the authors of Ref. 9 speculate that it is possible that under the conditions for low hydroxylation, two-phase catalysis could promote the formation of hydroxy groups clustered in one side of the cage because the reaction takes place mainly at the aqueous/solvent interface.

At this point, we would like to comment that theoretical calculations could be a valuable tool in order to shed some light into the previous controversy since, through direct comparison of theoretical and experimental data, it could be possible to elucidate some structural aspects of the synthesized individual molecular units leading to the monolayer formation. In this respect, we would like to say first that, within our theoretical framework, we have always obtained that random distributions of OH species on the C_{60} surface, as the ones proposed by Chiang *et al.*,[8] correspond to very unfavorable arrays. In particular, for 12 adsorbed OH groups, the random configuration of adsorbates has been found to be 1.6 eV less stable when compared with our most stable structure in which we have the coexistence of two opposite $(OH)_7$ and $(OH)_5$ hydroxyl clusters on the carbon surface. On the other hand, our results presented in Fig. 3 also show that the formation of molecular islands on C_{60} seems to be a more general feature of the carbon substrate, being independent of the presence of air-water interfaces and in qualitative agreement with the patchy behavior observed on the C_{60} surface for different atomic as well as molecular species. In this respect, it is important to comment that recent time-of-flight mass spectrometry and photoelectron spectroscopy experiments by Palpant *et al.*[31] have provided evidence of a similar clustering on the C_{60} surface where, in that case, Au atoms preferably form a Au_N cluster (for $N=0$ to 6) rather than a layered structure spread over the carbon cage. In addition, Dugourd *et al.*[32] have measured the electric polarizability of $C_{60}Na_n$ clusters in the range of $1 \leqslant n \leqslant 34$ and have concluded that their experimental data are consistent with the formation of a sodium droplet on the surface of the fullerene, an atomic configuration that has been later on confirmed by the theoretical calculations of Roques and co-workers.[33] Finally, Mixteco-Sánchez and Guirado-López[34] have found that thiol adsorption on C_{60} induces also the formation of molecular islands on the carbon surface, where the island size and shape has been found to critically depend on the length of the adsorbed species.

It is important to comment that, due to the highly anisotropic carbon network that we have obtained for the optimized $C_{60}(OH)_{9\text{-}12}$ structures, we estimate that the formation of Langmuir films with the use of molecular units as the ones shown in Fig. 3(e) or 3(f) would lead to a monolayer thickness of ~ 10.5 Å, where the presence of the two opposite hydroxyl clusters contributes significantly to the effective molecular diameter of the sample. Actually, our calculated diameter is not far away from the value of 11 Å estimated by Rincón *et al.*[9] or from the 12 ± 2 Å reported by Chiang and co-workers[8] for monolayers of $C_{60}(OH)_{12}$.

In order to furthermore corroborate the presence of hydroxyl islands on the C_{60} surface we show in Fig. 4 the calculated intensities of the vibrational frequencies of the $C_{60}(OH)_{10}$ compound by considering various relevant molecular configurations for the exterior hydroxyl groups, namely, ten OH molecules randomly distributed on the surface (configuration I), aggregated on one side of C_{60} (configuration II), and assuming the coexistence of two opposite hydroxyl clusters on the carbon structure, having seven and three molecules, which actually corresponds to our lowest-energy array (configuration III). We have chosen the $C_{60}(OH)_{10}$ structure as a representative example since it corresponds approximately to the degree of hydroxylation at which Rincón *et al.*[9] have synthesized stable Langmuir films and for which they have performed also infrared spectroscopy measurements in order to analyze the vibrational properties of the sample. As is well known, the precise details of the vibrational spectra (i.e., intensity and positions of the peaks) of $C_{60}(OH)_n$ fullerenes are expected to be very sensitive to the chemical bondings, to the number and distribution of the adsorbed molecules, as well as to the interactions among them. On the other hand, even if experimental and theoretical spectra are not strictly comparable, the possible existence of similar features in both distributions could be very helpful in elucidating the probable molecular structure of the adsorbed OH groups.

From Fig. 4(a) we can see that, for a random array of hydroxyl molecules (configuration I) our calculations indicate the presence of a very narrow and isolated distribution centered around 3670 cm^{-1}, which corresponds to the well-known stretching O-H mode already shown in Fig. 1. The existence of this narrow distribution is physically expected in such separated (almost noninteracting) array where the ad-

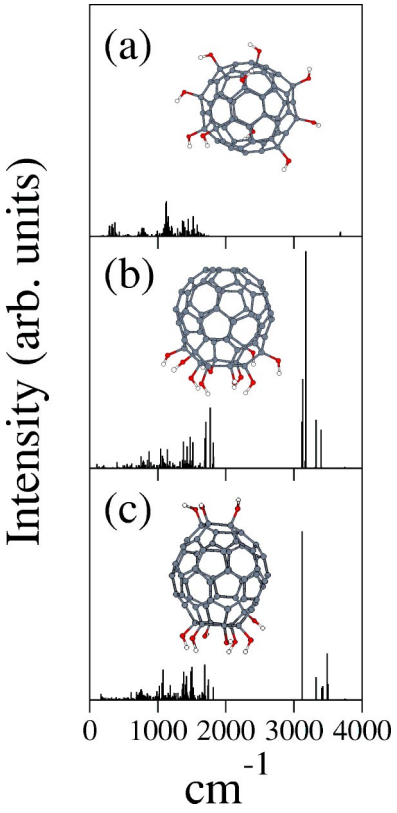

FIG. 4. Intensities of the calculated vibrational frequencies for various $C_{60}(OH)_{10}$ isomers. (a) OH molecules randomly distributed, (b) clustered on one side, and (c) as two opposite $(OH)_7$ and $(OH)_3$ hydroxyl clusters on the carbon surface.

sorbates perform thus independent vibrations, contributing with similar values to the intensity of the O-H stretching mode. However, when considering the existence of hydroxyl clusters on the surface, as the ones shown in Fig. 3, we expect that the coupling between adjacent OH molecules will lead to completely different vibrational features from those seen in the uncoupled system. In fact, we note from Figs. 4(b) and 4(c) that the narrow distribution obtained in Fig. 4(a) for the O-H stretching mode is now decomposed into several peaks, leading to the existence of a broadband which expands the frequency range from $\sim$3100 to 3750 cm^{-1}, and which can be considered as a clear signature of the presence of $(OH)_n$ clusters on the C_{60} surface. Furthermore, we can appreciate also sizable differences between the vibrational spectra of configurations II [Fig. 4(b)] and III [Fig. 4(c)] which clearly indicates how more subtle changes in the local organization of the adsorbates can also induce significant variations in the vibrational properties (intensity and position of the peaks) of the molecule. In fact, when comparing the various distributions of modes shown in Fig. 4 with the infrared spectroscopy measurements performed by Rincón *et al.*[9] on low hydroxylated C_{60} compounds we can see that the broad and asymmetric absorption band obtained around 3450 cm^{-1} in their IR spectrum is more in agreement with the presence of OH groups aggregated on C_{60} rather than randomly spread on the carbon surface.

As is well known, the structural rearrangements and energetics of low hydroxylated fullerenes already discussed in the previous paragraphs result from a delicate balance between the electronic and geometrical details present in the particles. Consequently, in the following, we analyze various of these factors that could be at the origin of the observed relative stability between the different configurations. First, it is interesting to correlate the observed equilibrium configurations for low coverages in Fig. 3 to the precise details of the electronic spectrum around the Fermi energy. As is well known, previous studies[35] have shown that, for C_{60} and C_{70}, large fragmentation energies are accompanied by large HOMO-LUMO energy gaps, both quantities being strongly correlated to the extraordinary abundance of these two fullerenes. In fact, as we can see from Fig. 5, both the stability of the molecular hydroxyl cluster $(1 \leqslant n \leqslant 7)$ as well as the structural transition leading to the coexistence of two opposite $(OH)_n$ islands $(8 \leqslant n \leqslant 14)$ follow this simple electronic argument, being in general [with the exception of the $C_{60}(OH)_{10}$ structure] the atomic configurations with the largest HOMO-LUMO energy separation the most stable arrays.

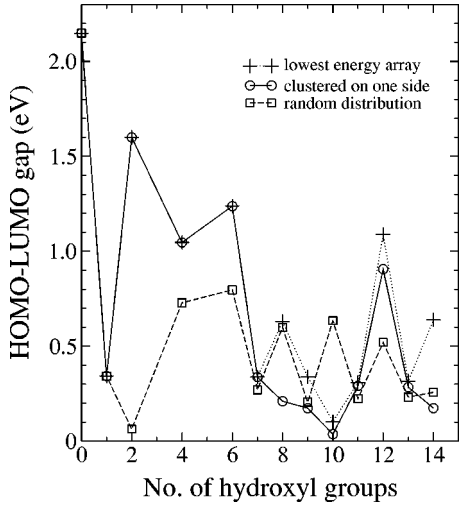

FIG. 5. Calculated HOMO-LUMO energy separation Δ_{HL} in eV for $C_{60}(OH)_N$ compounds at low coverages.

As already noticed from the single adsorption results, OH bonding on the C_{60} surface reduces the HOMO-LUMO energy gap from 2.14 eV (obtained for the uncovered cage) to 0.34 eV for the C_{60}-OH structure. However, with increasing the OH coverage, sizable additional modifications all along the electronic spectra are observed consisting of changes in the ordering of the eigenvalues, splitting of many of the energy levels that are degenerate in the bare C_{60}, together with various HOMO-LUMO gap reopenings and closings as the ones shown in Fig. 5. This complex behavior is mainly due to the considerable distortions produced on the carbon surface (see Fig. 3) which lowers the symmetry of the molecular structure, to the sizable variations in the local electron occupancies in the system, as well as due to the appearance of several additional electronic states around the Fermi energy induced by the precise location and number of the adsorbed OH groups on the carbon surface. This is clearly illustrated in Fig. 6 where we plot the electronic energy levels of the 16 sets of occupied molecular orbitals with the highest energies

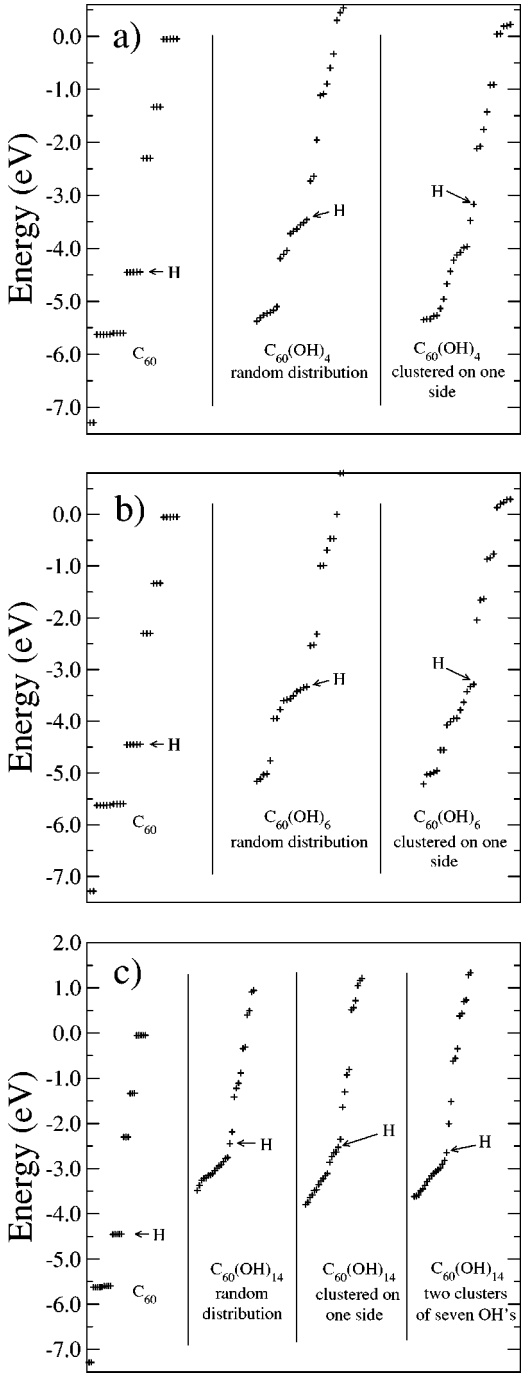

FIG. 6. Effects of the adsorption of OH molecules on the energy level of the HOMO and the 16 occupied energy levels below it as well as on the 11 unoccupied energy levels above it for (a) $C_{60}(OH)_4$, (b) $C_{60}(OH)_6$, and (c) $C_{60}(OH)_{14}$ compounds.

and of the 11 sets of unoccupied molecular orbitals with the lowest energies for 4, 6, and 14 randomly adsorbed OH species as well as when clustered on one or both sides of the C_{60} cage. For the sake of comparison we show also the corresponding energy-level distribution for the C_{60} molecule. From both figures we observe that the degeneracy of the spectrum for the uncovered cage (five degenerated HOMO and three-times degenerated LUMO) is considerably modified upon OH adsorption and that the HOMO and LUMO

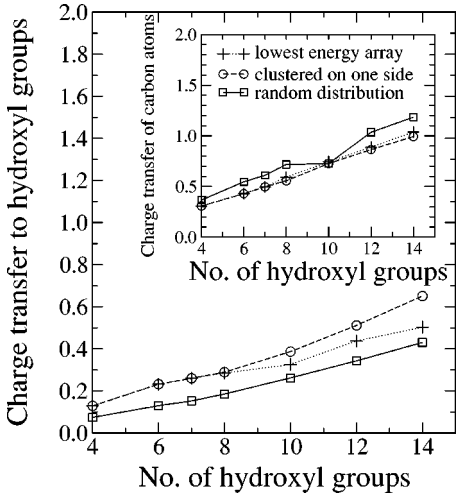

FIG. 7. Behavior of the total charge transfer from the C_{60} cage to the OH groups as a function of coverage for both clustered and random arrays. In the inset we show similar results but for the total amount of charge missing on the carbon atoms involved in the bonding.

levels are now placed in a region with a different distribution of energy states. As in previous cases, these new states are mainly of oxygen $2p$ character and are found to be strongly coupled with the $2p$ valence states of the carbon atoms of the cage, significantly changing as a consequence the conductivity of the OH-C_{60} compounds. By comparing Figs. 6(a)–6(c) we can clearly see also that, as a function of the number and location of the adsorbed hydroxyl groups, the energies of the considered occupied and unoccupied molecular orbitals can be significantly raised or lowered, leading to the existence of contrasting spectra and to dramatic changes in the degeneracy of the energy-level distribution. In fact, our results reveal that these level splittings are larger for four and six OH molecules clustered on the carbon cage as well as for 14 OH groups forming two opposite $(OH)_7$ islands on the fullerene surface (which are the type of adsorbed phases leading to the highest deformed molecular structures and to the most stable arrays) than for randomly distributed species, a difference that may be attributed to Jahn-Teller instabilities in the more symmetrical structures. However, despite this complex dynamics of the electronic states we can appreciate that, as a general tendency, the atomic configurations with the less degenerated spectra and largest HOMO-LUMO energy separation correspond to the most stable arrays.

Local electron occupancies are also of fundamental importance in determining the global properties of a system. In situations where there is a redistribution of valence electrons and/or charge transfer, analysis of the occupations of each one of the atoms involved in the bonding can provide us also with relevant information concerning the electronic properties and energetics. In Fig. 7 we show both the total amount of charge transferred to the OH groups as well as (in the inset) the total charge missing in the carbon atoms of the cage directly involved in the bonding which, as already stated in the previous paragraphs, are the atoms with the largest deviation from the bulk valence state ($n=4.0$), as a function of the adsorbed OH groups. From the figure we note

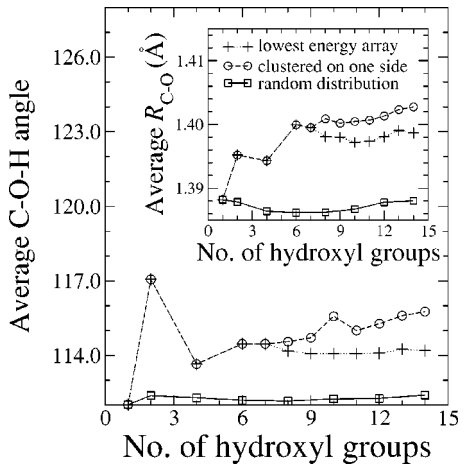

FIG. 8. Calculated average C-O-H tilting angle and average C-O bond length (inset), $R_{C\text{-}O}$, for $C_{60}(OH)_N$ compounds at low coverages.

that, as the coverage increases, the total $C_{60} \rightarrow OH$ charge transfer increases linearly for both clustered and random arrays and where the self-consistency of the distribution yields a charge transfer explicitly dependent on the adsorbed geometry. In fact, we note that, in the range of $8 \leqslant n \leqslant 14$, the electron-accepting character of the OH groups diminishes in our most stable configurations, when compared with the adsorbed phase in which the hydroxyl molecules are all clustered on one side of the cage, clearly reducing in the former the repulsive interactions between the neighboring OH species. On the other hand, the significant amount of charge transferred to the adsorbates is consistent with the sizable amount of charge missing in the carbon atoms directly involved in the bonding (see the inset) where values as large as $1\bar{e}$ are observed. This result obviously induces the existence of a highly repulsive environment in a localized region of the cage, due to the proximity of the various C^+ ions, originating C-C bond-length expansions as large as 14% in order to lower the total energy of the system.

We believe that the behavior of the charge transfer as a function of coverage obtained in Fig. 7 is also directly related with the noticeable variations in the energy-level spectra shown in Figs. 5 and 6, since the observed energy shifts of the eigenvalues around the HOMO (that are mainly of oxygen $2p$ character) will strongly depend on the amount and local redistribution of the electronic charge in the OH group which is, as we have shown in Fig. 7, continuously changing with increasing the number and location of the adsorbed species.

Even though Coulomb repulsion play an important role when the OH molecules are bonded to the carbon surface [see Figs. 3(a)–3(f)], where the adsorbates are found to be effectively charged and close to each other, we believe that quantum effects such as the degeneracy of the energy-level distribution, the open or closed character of the electronic shells, as well as the magnitude of the HOMO-LUMO energy separation (discussed in the previous paragraphes) enhance the stability in a local way overcoming the sizable contributions of the electrostatic repulsive interactions, being thus the major factor that determines the precise geometrical details of the adsorbed phases on the carbon surface.

In Fig. 8, we show the average orientation of the C-O-H angle as well as (in the inset) the evolution of the average C-O bond length, $R_{C\text{-}O}$, as a function of coverage for three different types of growth sequences, namely, OH molecules randomly distributed on the surface, aggregated on side of C_{60}, and considering the presence of two opposite hydroxyl clusters of different sizes on the carbon structure. We would like to comment that, in all our optimized structures, the OH molecules have been found to be tilted away from the surface normal, as in the isolated case [see Fig. 3(a)], but with a more complex distribution of C-O-H angles, ranging from 113° to 117°. Interestingly we note from Fig. 8 that our lowest-energy arrays shown in Fig. 3 are characterized by the presence of a well-defined C-O-H tilting angle of ~114°. This is in qualitative agreement with the results obtained in extended surfaces, where the various adsorbed phases that can be stabilized as a function of coverage are characterized by a high degree of molecular order. However, even if our results indicate that in our lowest-energy configurations the individual OH groups are adsorbed with a preferred C-O-H angle, we note that the relative orientations between neighboring molecules are not correlated, leading to the formation of orientationally disordered hydrophilic domains on the C_{60} surface [see Figs. 3(a)–3(f)]. Concerning the evolution of the average C-O bond length in our most stable arrays we can see an increasing behavior for $R_{C\text{-}O}$ with increasing coverage and that the curve appears to saturate for seven or more adsorbed OH's. From Fig. 8, it is important to remark also the physically expected almost constant behavior and reduced values in both the tilting angle and the C-O bonds lengths obtained for randomly distributed (almost noninteracting) molecules, as well as the increasing behavior in both average C-O-H angles and $R_{C\text{-}O}$ distances for OH groups clustered on one side of C_{60}, which clearly indicates that repulsive interactions play an important role in determining the overall adsorbed molecular structure.

Obviously, the specific locations and orientations of the adsorbed molecules have a profound impact on the adsorption energies and on the structural properties of the system, both quantities playing a fundamental role in explaining the relative stabilities and structural transitions observed as a function of coverage. Consequently, we show in Fig. 9 the calculated values for the adsorption energy E_{ads} [see Eq. (1)] as a function of coverage for OH molecules randomly distributed on the surface, aggregated on side of C_{60}, and considering the presence of two opposite hydroxyl clusters of different sizes on the carbon structure. From the figure we can see that, at very low coverages $(1 \leqslant n \leqslant 6)$, the configurations with the highest adsorption energies correspond to the adsorbed molecules which aggregate on one side of the carbon cage. In particular, it is important to remark the considerable enhancement of E_{ads} for two and three OH's adsorbed on adjacent carbon atoms of the C_{60} structure, when compared with the noninteracting array, which is consistent with the formation of molecular islands on the carbon surface. For $n \geqslant 8$ we note that subsequent OH aggregation on one side of the C_{60} is prevented since we observe a notable increase in

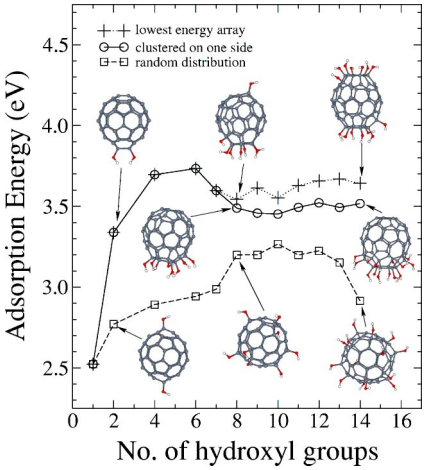

FIG. 9. Calculated adsorption energies E_{ads} in eV for low hydroxylated $C_{60}(OH)_N$ compounds.

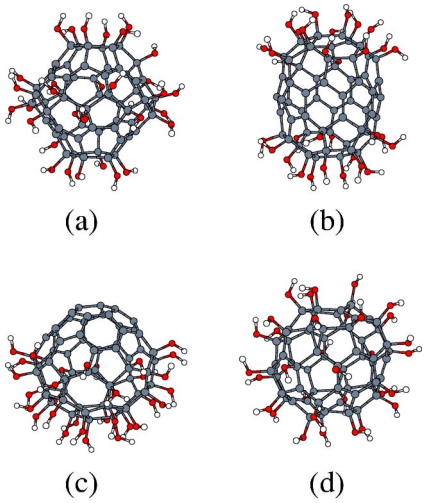

FIG. 10. Optimized MNDO configurations for 32 OH molecules adsorbed on C_{60}. (a) Lowest-energy array, (b) coexistence of two opposite $(OH)_{16}$ clusters, (c) OH groups clustered on one side, and (d) randomly distributed on the surface.

E_{ads} when OH adsorption starts to take place now on the opposite side of the fullerene cage. In particular, for $n=8$, we note a relatively small energy difference ($\sim$0.4 eV) between configurations II and III (as referred to in the figure) which is of fundamental importance in order to quantify the magnitude of the diffusion barriers of the adsorbates on the carbon surface. As is well known, small energy differences would lead to the formation of a highly dynamical two-dimensional system in which several configurations can be present in the sample in the time scale of the experiment, a fact that can lead to a wide variety of macroscopic behaviors. With increasing coverage ($n \geqslant 9$), we note that energy differences between all our considered configurations become more pronounced, clearly defining the existence of a well-defined growth sequence. On the other hand, it is important to remark the considerable reduced values of E_{ads} for randomly distributed molecules, clearly indicating that this bonding situation is very unstable.

In order to analyze the possible geometric structure of the adsorbed hydroxyl molecules leading to the complete solubility of the C_{60} molecule, we present in Fig. 10 the fully relaxed MNDO structures for highly covered $C_{60}(OH)_{32}$ compounds. In these cases, we have performed also a symmetry unconstrained minimization calculation for several initial configurations of the OH groups. First, following our results shown in Fig. 3(f) we have assumed that, with increasing coverage, the two opposite islands are able to grow on the carbon structure in both symmetric and asymmetric ways. Second, we consider that molecular clusters made of seven OH groups define a critical size (as already discussed) for the extension of the hydrophilic domains on the fullerene surface and we propose thus to separate the two coexisting $(OH)_7$ clusters shown in Fig. 3(f) by a ringlike configuration of 18 OH groups around C_{60}. Finally, we compare the previous configurations with 32 hydroxyl molecules randomly distributed on the surface as well as aggregated on one side of the carbon structure. Interestingly, we have found from our total-energy calculations that our most stable array, which corresponds to the two opposite $(OH)_7$ clusters separated by a ring-like configuration of OH molecules [see Fig. 10(a)], is the only one in which the individual OH groups are able to adsorb also with the preferred C-O-H tilting angle of 114° already observed in the molecular structures shown in Fig. 3. With respect to the simultaneous growth of the two opposite hydroxyl clusters we have found that the existence of asymmetric arrays corresponds to very unfavorable configurations, and finally, OH groups clustered on one side or randomly distributed on the surface are found to be $\sim$6 eV less stable when compared with the $C_{60}(OH)_{32}$ compound shown in Fig. 10(a).

Finally, we would like to point out that the knowledge of the precise geometrical configuration of the exterior OH groups at different coverages is also of fundamental importance since it is expected to strongly influence the particle's interaction with its surroundings, directing thus the self-organization and packing of the C_{60} molecules when deposited on solid substrates or at air-liquid interfaces. The properties of molecular $C_{60}(OH)_n$ monolayers will be thus not only determined by the intrinsic properties of the individual building blocks but also by the intermolecular interactions among them. At this respect we believe that the sizable amount of carbon surface exposed by our lowest-energy arrays shown in Fig. 3 could allow some polymerization processes that might lead to interesting transport properties in the sample. On the other hand, highly hydroxylated structures as the ones shown in Fig. 10(a), which are coated with a molecular overlayer that insulates the individual C_{60} molecules from each other, might not be well suited for producing highly conducting films. In addition, we must say that subsequent C_{60} deposition should be strongly influenced by the precise chemical nature of the outermost surface atoms exposed by the $C_{60}(OH)_N$ monolayer. It is clear then that the use of molecular units as the ones shown in Fig. 3(c) or 3(f), which exhibit hydrophobic and hydrophilic opposite regions, respectively, will serve as growth seeds for completely different multilayered structures.

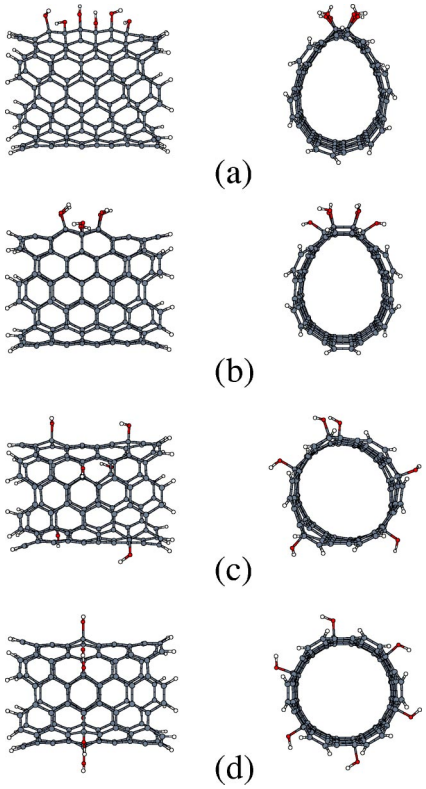

FIG. 11. Optimized MNDO configurations for six OH molecules adsorbed in a (6,6) $C_{120}(OH)_{24}$ nanotube. In the right column, we show the side view of the calculated equilibrium configuration.

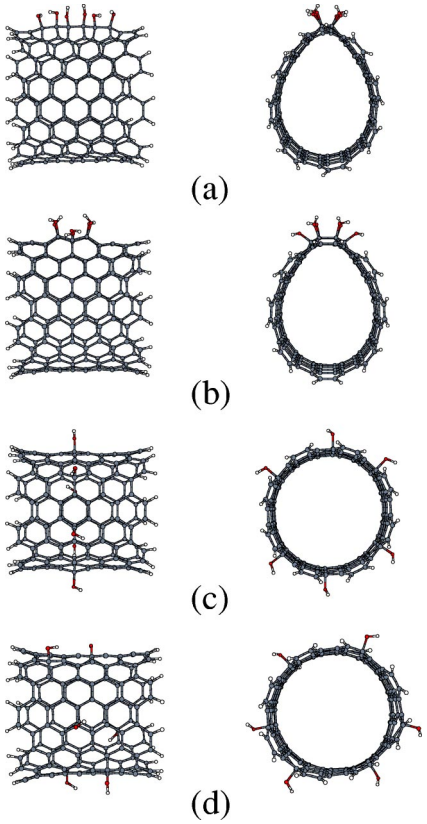

FIG. 12. Optimized MNDO configurations for six OH molecules adsorbed in a (8,8) $C_{160}(OH)_{32}$ nanotube. In the right column, we show the side view of the calculated equilibrium configuration.

B. Low hydroxylated carbon nanotubes

In this section, we present the molecular ordering of OH groups on the external surface of finite length (6,6) and (8,8) SWNT's in order to analyze both the influence of curvature and tube's diameter on the C-OH bonding features, as well as the different adsorbed phases that can be obtained as a function of coverage and initial configurations of the adsorbates. The cluster models for our SWNT's are (6,6) and (8,8) armchair open-ended tubes containing 120 and 160 carbon atoms, respectively, where the dangling bonds at the ends are tied off with hydrogen atoms yielding $C_{120}H_{24}$ and $C_{160}H_{32}$ structures. In this case, we have performed also a symmetry unconstrained minimization procedure for several initial configurations of the adsorbates in order to cover the possible binding environments of the OH group, namely, (1) uniformly distributed on the surface (I), (2) a ringlike configuration around the tube (II), (3) clustered on the surface (III), and (4) forming one-dimensional array along the tube (IV).

In Figs. 11 and 12 we present, as representative results, the fully relaxed MNDO structures for six OH molecules adsorbed in our $C_{120}H_{24}$ and $C_{160}H_{32}$ tubes for the considered initial configurations I, II, III, and IV defined in the previous paragraph. In Figs. 11(a) and 12(a) we present the lowest-energy array, together with some metastable configurations in Figs. 11(b)–11(d) as well as in Figs. 12(b)–12(d), being relatively close in energy (energy differences as large as 1 eV), but having completely different structural features. As in Figs. 3 and 10, we find that the individual hydroxyl molecules prefer to bind also in the atop configuration with a C-O-H tilting angle ranging from 111° to 115°. From both figures it is important to note that six OH molecules adsorbed on (6,6) and (8,8) carbon nanotubes prefer to be organized (independent of the diameter) in a compact zigzag configuration along the tubes [see Figs. 11(a) and 12(a)], and that it is considerably unfavorable for them to be attached on adjacent carbon atoms forming a cluster array, as has been found for the spheroidal structure (see Fig. 3). It is thus clear that the different curvature of the carbon substrate causes a rehybridization of the bonding orbitals inducing completely different adsorbed phases. In fact, by calculating the adsorption energies E_{ads} for the most stable $C_{120}H_{24}$-6OH and $C_{160}H_{32}$-6OH compounds, shown in Figs. 11(a) and 12(a), we have found values of 3.22 and 3.03 eV, respectively, being both of them smaller when compared with the value obtained for the C_{60}-6OH molecule (see Fig. 9), which clearly indicates that the spheroidal structures are most appropriate substrates for OH adsorption. We would like to point out that the extention of the one-dimensional molecular arrays observed in Figs. 11(a) and 12(a) can be accurately controlled by using carbon nanotubes of different lengths. As is well known, the latter can be easily prepared by practically cutting nearly endless ropes of nanotubes with the use of ion bombardment or prolongated sonication techniques.[13] With the resulting pieces (fullerene pipes) a stable nanotube suspension can be formed, which in turn can be used to perform

a length-selected precipitation into a solid substrate in which subsequent deposition of various molecules can be performed.

From Figs. 11 and 12 we can observe two kinds of structural deformations, namely, local and distributed over the length of the tube. The first ones [Figs. 11(c), 11(d), 12(c), and 12(d)] are characterized by an outward relaxation of the carbon atoms directly involved in the bonding, which also induces some appreciable distortions only in the neighboring atoms around the adsorption site. In the second case [Figs. 11(a), 11(b), 12(a), and 12(b)], a clear deviation from circular tube is observed, which actually propagates all along the carbon structure. These sizable extended nonuniform radial deformations significantly modify the energy-level distribution all along the electronic spectra, but still preserve the well-known conducting character of the armchair nanotubes (HOMO-LUMO gaps of the order of 0.7 eV). Furthermore, they are of crucial importance in determining the relative stabilities between the different adsorbed configurations. Actually, by performing a restricted optimization procedure in which the carbon atoms of the nanotube are not allowed to relax upon OH adsorption, we have found a dramatic reorganization in the energy ordering of the structures shown in Fig. 11, where now the ringlike configuration of the adsorbed hydroxyl groups [see Fig. 11(d)] is more stable than the linear array (by 2 eV). This result is very important, and clearly shows the relevance of performing unrestricted energy minimization procedures in order to avoid misleading results. Finally, additional calculations on a $C_{192}H_{32}$-6OH compound reveal that these global nonuniform radial deformations are less pronounced with increasing the length of the carbon arrays, however they still lead to the existence of localized regions which exhibit clear deviations from the circular cross section characterizing the structure of uncovered nanotubes. Of course, it will be interesting to determine also whether these structural deformations and significant modifications to the electronic spectra are sensitive to the chiral indices of the nanotubes (n,m), which will give the opportunity to fabricate interesting molecular conductors with tunable properties.

Finally, it is important to comment that our lowest-energy configurations shown in Figs. 11(a) and 12(a) are consistent with recent experimental investigations which have demonstrated that titanium atoms deposited on SWNT's are capable of forming also continuous quasi-one-dimensional arrays.[36] Theoretical first-principles calculations[37] have obtained strong binding energies for these adsorbed Ti chains (ranging from 1.62 to 2.04 eV) and have suggested the possibility that, by using titanium as a buffer layer on nanotubes, continuous nanowires of practically any metal can be obtained. However, our results in Figs. 11(a) and 12(a) seem to reveal that the stabilization of linear arrays could be a more general feature of these type of carbon substrates, opening thus the possibility to fabricate quasi-one-dimensional metal, organic, as well as semiconducting nanostructures when deposited on the external surface of carbon nanotubes.

IV. CONCLUSIONS

In this work we have presented a systematic study, by combining semiempirical and DFT approaches, of the structural, electronic, and vibrational properties of OH molecules adsorbed on the external surfaces of C_{60} as well as on finite length (6,6) and (8,8) carbon nanotubes. A considerable insight is now available about the local organization of the molecules on the carbon surfaces, and in particular, concerning the factors controlling the competition between different growth sequences. At low coverages, we have found that the hydroxyl molecules prefer to aggregate as a cluster on one side of the C_{60} cage, a result that seems be of fundamental importance in explaining the stability of C_{60} monolayers at the air-water interface observed by several authors. In fact, a direct comparison between our calculated vibrational spectra and the reported infrared spectroscopy measurements for low hydroxylated C_{60} compounds seems to support the hydroxyl island formation on the spheroidal carbon surface predicted in this work. With increasing OH coverage, quantum effects and the increasing repulsive interactions induce sizable molecular displacements, as well as significant reorganization of the adsorbates on the surface, leading to the coexistence of hydroxyl islands as well as to the formation of ringlike configurations on C_{60}. We have found that the considerable distortions observed on the C_{60} cage upon OH adsorption lead to the development of a highly anisotropic carbon network, clearly revealing the considerable flexibility of the C_{60} structure, and whose effective diameter ($\sim$10.5 Å) is in fact of the order of the measured thickness of the synthesized $C_{60}(OH)_{9-12}$ monolayers. In our tubelike configurations we have found, in qualitative agreement with the recent synthesis of metal nanowires on the surface of SWNT's, the stabilization of molecular quasi-one-dimensional arrays, which explicitly reveals the curvature and site dependence of the C-OH bonding features. Finally, we would like to conclude by saying that due to the complex specific arrangements that we have obtained for the OH species at different coverages, as well as for different geometrical details of the underlying carbon substrate, it seems to be possible to effectively use fullerene materials as templates for controlling the locations (e.g., create molecular islands or one-dimensional arrays of different materials on their surfaces), and probably also the orientation, of a wide variety of atomic and molecular species, leading to the formation of nanostructured materials with designed properties.

ACKNOWLEDGMENTS

We thank Dr. Marina Rincón and Dr. Jaime Ruiz-García for valuable discussions. J.G.R-Z would like to acknowledge the financial support from CONACyT (México) (Grant No. 129983). R.A.G-L would like to acknowledge the financial support from Fondo de Apoyo a la Investigación (UASLP) through Grant No. C02-FAI-11-20.81.

*Electronic address: gusro@ifisica.uaslp.mx
†Electronic address: guirado@ifisica.uaslp.mx

[1] C. Prados, P. Crespo, J.M. González, A. Hernando, J.F. Marco, R. Gancedo, N. Grobert, M. Terrones, R.M. Walton, and H.W. Kroto, Phys. Rev. B **65**, 113405 (2002).
[2] Y.H. Gao and Y. Bando, Nature (London) **415**, 599 (2002).
[3] J. Kong, N.R. Franklin, C. Chou, M.G. Chaplin, S. Peng, K. Cho, and H. Dai, Science **287**, 622 (2000); H. Chang, J.D. Lee, S.M. Lee, and Y.H. Lee, Appl. Phys. Lett. **79**, 3863 (2001); R. Pati, Y. Zhang, S.K. Nayak, and P.M. Ajayan, *ibid.* **81**, 2638 (2002).
[4] A.C. Dillon, K.M. Jones, T.A. Bekkedahl, C.H. Kiang, D.S. Bethune, and M.J. Heben, Nature (London) **386**, 377 (1997); C. Liu, Y.Y. Fan, M. Liu, H.T. Cong, H.M. Cheng, and M.S. Dresselhaus, Science **286**, 1127 (1999); P. Chen, X. Wu, J. Lin, and K.L. Tan, *ibid.* **285**, 91 (1999); R.C. Gordillo, J. Boronat, and J. Casulleras, Phys. Rev. Lett. **85**, 2348 (2000); R.E. Barajas-Barraza and R.A. Guirado-López, Phys. Rev. B **66**, 155426 (2002).
[5] A.F. Hebard, M.J. Rosseinsky, R.C. Haddon, D.W. Murphy, S.H. Glarum, T.T.M. Palstra, A.P. Ramirez, and A.R. Kortan, Nature (London) **350**, 600 (1991).
[6] D.M. Guldi, M. Maggini, S. Mondini, F. Guérin, and J.H. Fendler, Langmuir **16**, 1311 (2000).
[7] M. De Seta, D. Sanvitto, and F. Evangelisti, Phys. Rev. B **59**, 9878 (1999); C. Cepek, I. Vobornik, A. Goldoni, E. Magnano, G. Selvaggi, J. Kröger, G. Panaccione, G. Rossi, and M. Sancrotti, *ibid.* **86**, 3100 (2001); S. Woedtke, A. Meeder, R. Adelung, R. Schwedhelm, L. Kipp, and M. Skibowski, *ibid.* **63**, 155401 (2001); M. Grobis, X. Lu, and M.F. Crommie, *ibid.* **66**, 161408 (2002).
[8] W.J. Liu, U. Jeng, T.L. Lin, S.H. Lai, M.C. Shih, C.S. Tsao, L.Y. Wang, L.Y. Chiang, and L.P. Sung, Physica B **283**, 49 (2000).
[9] M.E. Rincón, H. Hu, J. Campos, and J. Ruíz-García, J. Phys. Chem. B **107**, 4111 (2003).
[10] M. Mikawa, H. Kato, M. Okumura, M. Narazaki, Y. Kanazawa, N. Miwa, and H. Shinohara, Bioconjugate Chem. **12**, 510 (2001).
[11] D.W. Cagle, S.J. Kennel, S. Mirzadeh, J.M. Alford, and L.J. Wilson, Proc. Natl. Acad. Sci. U.S.A. **96**, 5182 (1999).
[12] J. Chen, M.A. Hamon, H. Hu, Y. Chen, A.M. Rao, P.C. Eklund, and R.C. Haddon, Science **282**, 95 (1998); S.S. Wong, E. Joselevich, A.T. Woolley, C.L. Cheung, and C.M. Lieber, Nature (London) **394**, 52 (1998).
[13] J. Liu, A.G. Rinzler, H. Dai, J.H. Hafner, R.K. Bradley, P.J. Boul, A. Lu, T. Iverson, K. Shelimov, C.B. Huffman, F. Rodríguez-Macías, Y.S. Shon, T.R. Lee, D.T. Colbert, and R.E. Smalley, Science **280**, 1253 (1998).
[14] K. Bedürftig, S. Völkening, Y. Wang, J. Wintterlin, K. Jacobi, and G. Ertl, J. Chem. Phys. **111**, 11 147 (1999).
[15] M.J.S. Dewar and W. Thiel, J. Am. Chem. Soc. **99**, 4899 (1977); **99**, 4907 (1977).
[16] S.H. Vosko, L. Wilk, and M. Nusair, Can. J. Phys. **58**, 1200 (1980).
[17] A.D. Becke, J. Chem. Phys. **98**, 5648 (1993).
[18] C. Lee, W. Yang, and R.G. Parr, Phys. Rev. B **37**, 785 (1998).
[19] D. Bakowies and W. Thiel, J. Am. Chem. Soc. **113**, 3704 (1991).
[20] K. Hedberg, L. Hedberg, D.S. Bethune, C.A. Brown, H.C. Dorn, R.D. Johnson, and M. de Vries, Science **254**, 410 (1991).
[21] M. Häser, J. Almlöf, and G.E. Scuseria, Chem. Phys. Lett. **181**, 497 (1991).
[22] H.P. Lüthi and J. Almlöf, Chem. Phys. Lett. **135**, 357 (1987).
[23] J. de Vries, H. Steger, B. Kanke, C. Manzel, B. Weisser, W. Kamke, and I.V. Hertel, Chem. Phys. Lett. **188**, 159 (1992).
[24] U. Zimmermann, A. Burkhardt, N. Malinowsky, U. Näher, and T.P. Martin, J. Chem. Phys. **101**, 2244 (1994).
[25] D.L. Strout, R.L. Murry, C. Xu, W.C. Eckhoff, G.K. Odom, and G.E. Scuseria, Chem. Phys. Lett. **214**, 576 (1993).
[26] M. J. Frisch, G. W. Trucks, H. B. Schlegel, G. E. Scuseria, M. A. Robb, J. R. Cheeseman, V. G. Zakrzewski, J. A. Montgomery, Jr., R. E. Stratmann, J. C. Burant, S. Dapprich, J. M. Millam, A. D. Daniels, K. N. Kudin, M. C. Strain, O. Farkas, J. Tomasi, V. Barone, M. Cossi, R. Cammi, B. Mennucci, C. Pomelli, C. Adamo, S. Clifford, J. Ochterski, G. A. Petersson, P. Y. Ayala, Q. Cui, K. Morokuma, D. K. Malick, A. D. Rabuck, K. Raghavachari, J. B. Foresman, J. Cioslowski, J. V. Ortiz, A. G. Baboul, B. B. Stefanov, G. Liu, A. Liashenko, P. Piskorz, I. Komaromi, R. Gomperts, R. L. Martin, D. J. Fox, T. Keith, M. A. Al-Laham, C. Y. Peng, A. Nanayakkara, M. Challacombe, P. M. W. Gill, B. Johnson, W. Chen, M. W. Wong, J. L. Andres, C. Gonzalez, M. Head-Gordon, E. S. Replogle, and J. A. Pople, GAUSSIAN98, Revision A.9 (Gaussian, Pittsburgh, PA, 1998).
[27] W.J. Hehre, R.F. Stewart, and J.A. Pople, J. Chem. Phys. **51**, 2657 (1969); J.B. Collins, P.v.R. Schleyer, J.S. Binkley, and J.A. Pople, *ibid.* **64**, 5142 (1976).
[28] J.S. Binkley, J.A. Pople, and W.J. Henre, J. Am. Chem. Soc. **102**, 939 (1980); M.S. Gordon, J.S. Binkley, J.A. Pople, W.J. Pietro, and W.J. Henre, *ibid.* **104**, 2797 (1982).
[29] K. Kobayashi and N. Kurita, Phys. Rev. Lett. **70**, 3542 (1993), and references therein.
[30] J.H. Weaver, J.L. Martins, T. Komeda, Y. Chen, T.R. Ohno, G.H. Kroll, N. Troullier, R.E. Haufler, and R.E. Smalley, Phys. Rev. Lett. **66**, 1741 (1991); R.W. Lof, M.A. van Veenendaal, B. Koopmans, H.T. Jonkman, and G.A. Sawatzky, *ibid.* **68**, 3924 (1992).
[31] B. Palpant, Y. Negishi, M. Sanekata, K. Miyajima, S. Nagao, K. Judai, D.M. Rayner, B. Simard, P.A. Hackett, A. Nakajima, and K. Kaya, J. Chem. Phys. **114**, 8459 (2001).
[32] Ph. Dugourd, R. Antoine, D. Rayane, I. Compagnon, and M. Broyer, J. Chem. Phys. **114**, 1970 (2001).
[33] J. Roques, F. Calvo, F. Spiegelman, and C. Mijoule, Phys. Rev. Lett. **90**, 075505 (2003).
[34] J.C. Mixteco-Sánchez and R.A. Guirado-López, Phys. Rev. A **68**, 053204 (2003).
[35] C.Z. Wang, B.L. Zhang, C.H. Xu, C.T. Chan, and K.M. Ho, Int. J. Mod. Phys. A **6**, 3833 (1992).
[36] Y. Zhang and H. Dai, Appl. Phys. Lett. **77**, 3015 (2000); Y. Zhang, N.W. Franklin, R.J. Chen, and H. Dai, Chem. Phys. Lett. **331**, 35 (2000).
[37] C.K. Yang, J. Zhao, and J.P. Lu, Phys. Rev. B **66**, 041403 (2002).